# A Simple Destriping Algorithm for MOS Images

Bryan A. Franz
SAIC General Sciences Corporation
NASA/SIMBIOS Project

## ABSTRACT

Due to variations in the relative response of the individual detectors on the MOS CCD array, along-track stripes are clearly visible in the imagery. Beyond aesthetics, such artifacts can contribute to confusion in the atmospheric correction process, particularly in the determination of aerosol type where band-to-band ratios must be used. For this reason, a simple filtering technique was developed which attempts to eliminate the detector-dependent variations while preserving the underlying structure of the images. The filtering algorithm is described, and results are presented showing application of the method to several MOS scenes.

## 1. Introduction

Any destriping method that derives corrections directly from the MOS imagery must attempt to distinguish the real structure in the scene from the variations induced by the relative sensitivity of the individual detectors. This is made difficult by the fact that the detector variability creates artifacts of similar spatial frequency to the in-water structure that MOS is attempting to measure. In the approach presented here, a cubic polynomial is used to model the low frequency variation generally associated with viewing geometry, while simple probability is relied upon to distinguish the higher frequency structure from the detector-induced variability. The following paragraphs describe the algorithm in detail.

## 2. Description of Algorithm

First, using any reasonable method, mask pixels that are contaminated by land or clouds to minimize sharp transitions in the image. In this analysis, a simple threshold on the 870-nm band is used to define the land/cloud mask. Defining $L_\lambda(i,j)$ as the observed radiance at wavelength $\lambda$ for detector i, scan j; set $L_\lambda(i,j) = 0.0$ when $L_{870}(i,j) > 2.0$ mW/cm$^2$/$\mu$m/sr.

Now, fit the unmasked pixels of each scan in the image to a cubic polynomial. This fitting function attempts to distinguish the large-scale variation across the image from the higher-frequency structure in the scene. So, for each scan j, compute a least-square fit to $L_\lambda(i,j)$ as a function of detector number, i.

$$F_j(i) = \Sigma\, C_k\, i^k,\ k=0..3$$

An example of this fitting process is shown in Figure 1a, where the triangles represent the observed radiances at 443 nm from each detector over a single MOS line, and the solid line shows the resulting fit for $F_j(i)$.

The next step is to compute a gain coefficient for each detector of each scan which relates the observed radiances to the fitted radiances.

$$g(i,j) = F_j(i) / L_\lambda(i,j)$$

A sample plot of g(i,j) as a function of detector number is shown for a single scan in Figure 1b, while Figure 1c shows the gain coefficients from all scans of one complete 384 x 384-pixel MOS scene.

If the smooth fit was a perfect representation of the large-scale variations in each scan, and there was no actual small-scale structure within the image, the g(i,j) of every scan would be identical for a given detector, and g(i,1) could be used to correct all scans for striping artifacts. In reality, we must estimate the destriping function by assuming that, for a given detector, real differences between the smooth fits and the observed radiances over many scans will average to zero, and any constant difference associated with the variation in detector sensitivity can thereby be recovered. To minimize the impact of large outliers when averaging g(i,j) over all j, the median is used to determine the average gain correction per detector.

$$G(i) = \text{median}(g(i,j), j=1..n)$$

The resulting G(i) represents the relative gain correction to be applied to detector i for all scans. This is shown as the solid line in Figure 1c. The destriped image, $L'_\lambda(i,j)$, can now be computed by application of G(i) to each scan.

$$L'_\lambda(i,j) = L_\lambda(i,j)\, G(i)$$

## 3. Discussion of Results

Figure 2 presents a MOS scene from the Western Mediterranean at 443 nm. The destriped image shows a significant reduction in detector-dependent variability with no obvious loss of in-water structure, and the difference image indicates that the destriping has induced no large-scale trends. Similar conclusions can be drawn from Figure 3, which shows results for a different scene at a different wavelength. Although this image is partially corrupted by clouds, the method still appears to successfully remove the detector striping.

In the filtering method described herein, the polynomial function acts as a spatial frequency threshold to distinguish low-frequency structure from high-frequency structure and stripes. The choice of this fitting function is critical to the success of the algorithm. If the function is not flexible enough to match the actual, large-scale variations in the scan direction, low-frequency stripes will be created in the filtered image. If the fitting function is too flexible, it will tend to follow the lowest frequency stripes and they will not be removed. A possible enhancement to this simple approach would be to allow the order of the polynomial fitting function to adapt to the low-frequency variability of the scene. For instance, the appropriate function could be determined by increasing the order of the fit until the $\chi^2$ stops changing significantly. Alternatively, the fitting function could be replaced by any other reasonable model of the large-scale structure, such as might be obtained by a low-pass filtering of the scan line.

One of the assumptions inherent in the derivation of this algorithm is that the striping artifacts are the result of a change in the relative sensitivity of the individual detectors. The adjustment was therefore defined as a relative gain correction (i.e., the size of the correction varies in proportion to signal level). Other approaches may assume that the effect is due to a change in the relative bias of the detectors, and

thus derive a correction to the detector offsets rather than the gains. Still other methods may attempt to model the corrections as a gain and offset, or some non-linear function of signal level.

Since the destriping algorithm described here has not been widely tested, no definitive claims can be made as to its general applicability and accuracy or its performance with respect to other methods. The algorithm was developed to minimize the uncertainties associated with detector-dependent variability within the atmospheric correction process, and it appears to work well in the scenes to which it was applied.

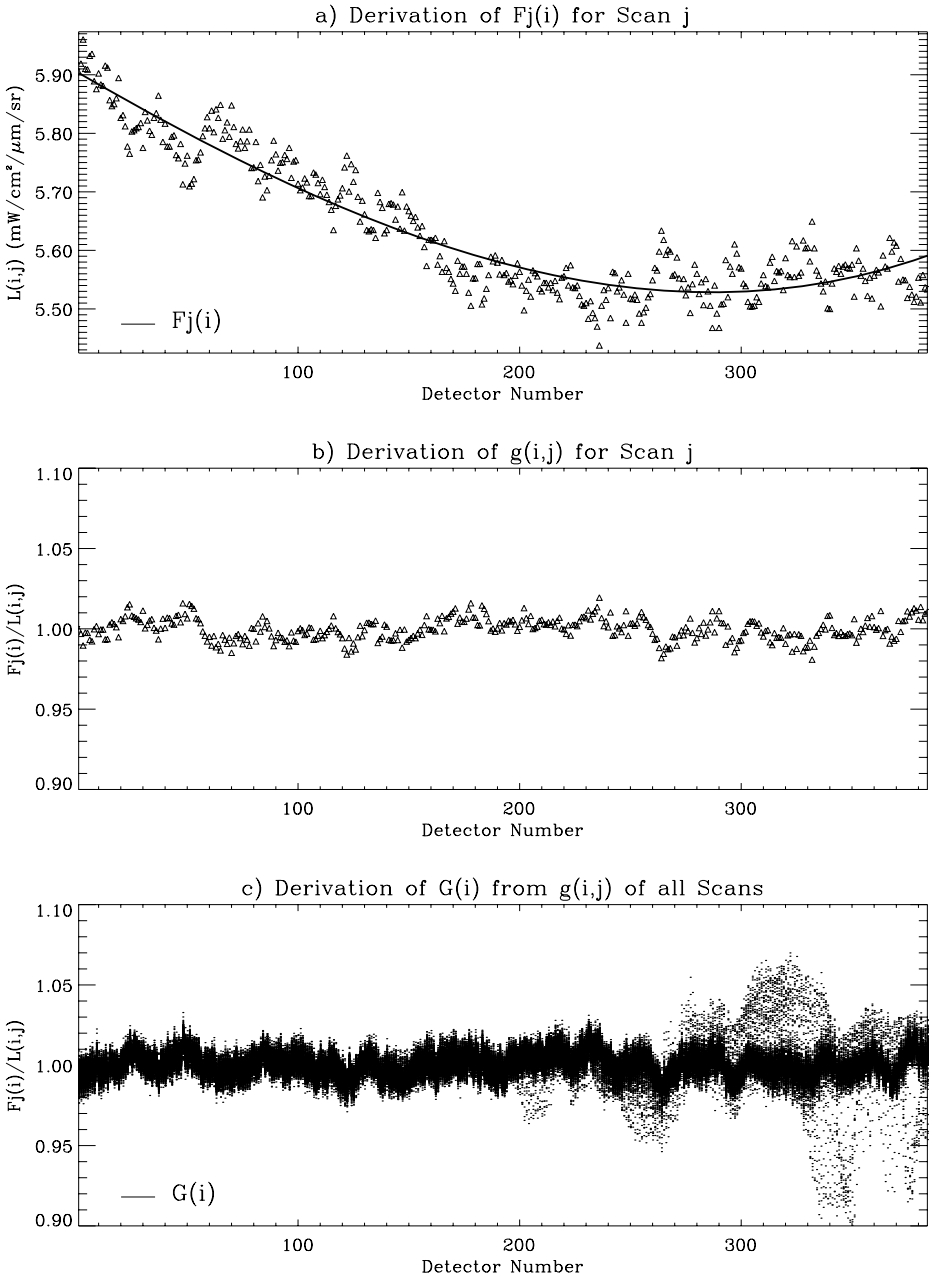


*Figure 1*: MOS Destriping Process for a Scene at 443 nm.

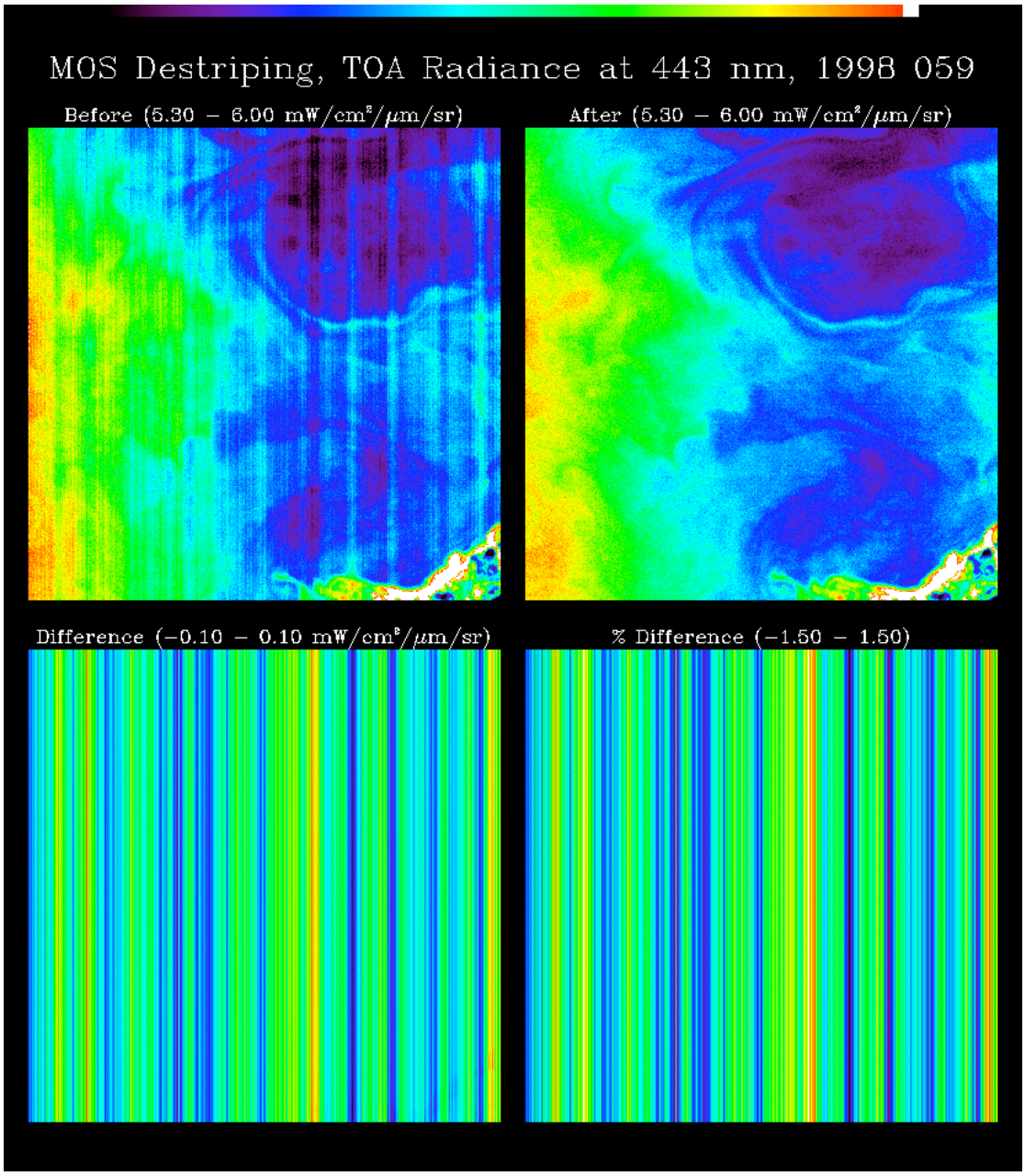
MOS Destriping, TOA Radiance at 443 nm, 1998 059
Before (5.30 – 6.00 mW/cm²/μm/sr)
After (5.30 – 6.00 mW/cm²/μm/sr)
Difference (–0.10 – 0.10 mW/cm²/μm/sr)
% Difference (–1.50 – 1.50)

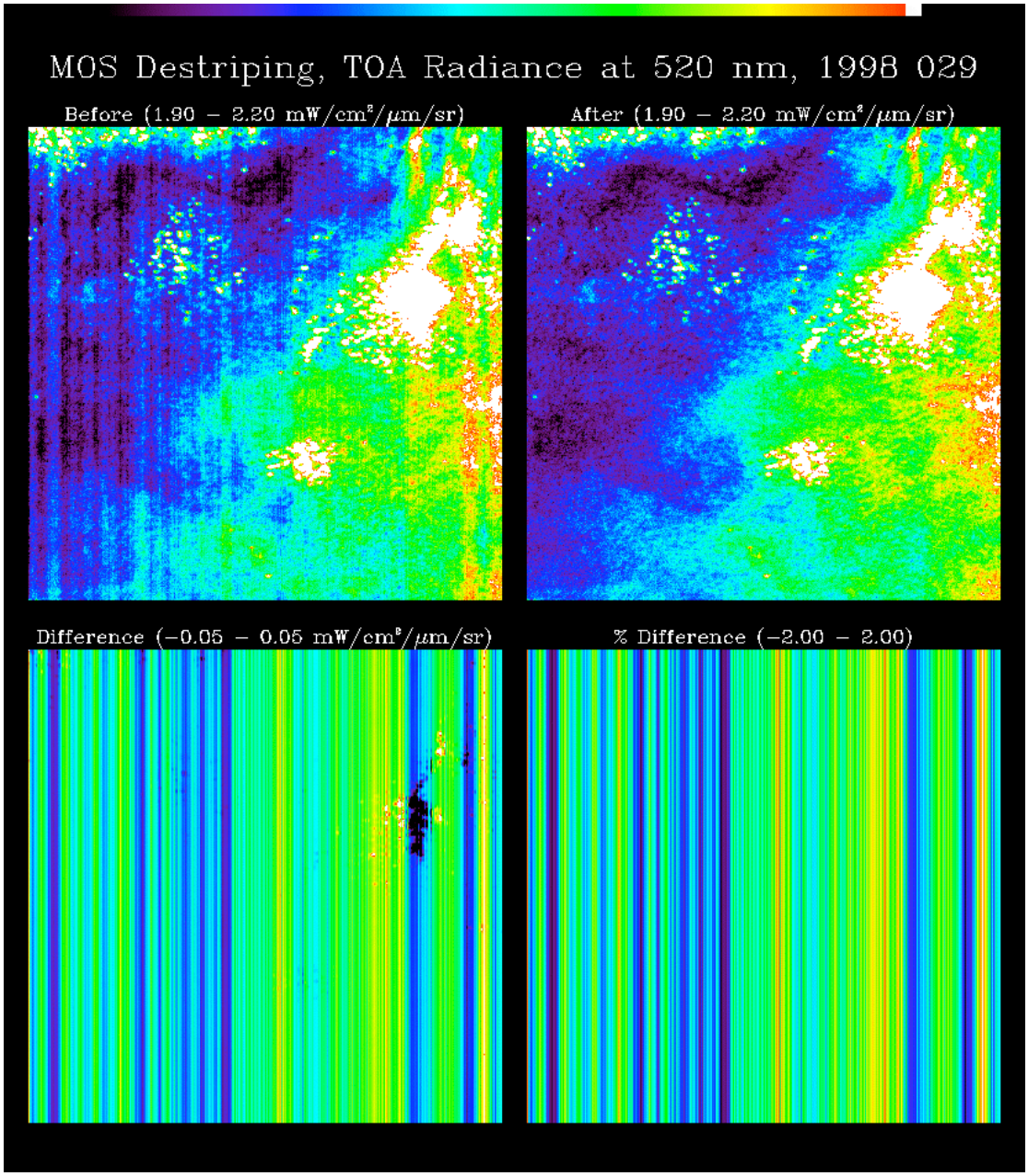


*Figure 3*: Image Destriping Example at 520 nm.

## Acknowledgment

Funding for this work was provided by the National Aeronautics and Space Administration through the Sensor Intercomparison and Merger for Biological and Interdisciplinary Oceanic Studies (SIMBIOS) project, under the direction of Dr. C. McClain. The author wishes to acknowledge Dr. Menghua Wang of the SIMBIOS project for his contributions to the development of the destriping algorithm, and Dr. A. Neumann and his colleagues at the DLR Institute for Space Sensor Technology for building the MOS sensor and providing the data and documentation that makes this work possible.

## References

1. Neumann, A., Walzel, T., Tschentscher, C., Gerasch, B., Krawczyk, H. “MOS-IRS Data Processing, Software and Data Products (Preliminary Documentation),” DLR Institute for Space Sensor Technology.
2. Neumann, A. “Spaceborne Imaging Spectrometers for Ocean Color Remote Sensing, MOS-PIRODA and MOS-IRS,” IOC Ocean Color Workshop, Victoria B.C. 1995.
3. Zimmrmann, G., Neumann, A., “The Spaceborn Imaging Spectrometer MOS for Ocean Remote Sensing,” in *Proceedings of the 1st International Workshop on MOS-IRS and Ocean Colo*r, pp. 1-9, DLR Institute for Space Sensor Technology. Berlin 1997.

*Figure 2*: Image Destriping Example at 443 nm.

*Figure 3*: Image Destriping Example at 520 nm.